Geophysical Research Letters

RESEARCH LETTER
10.1029/2023GL105159

New Insights Into Active Faults Revealed by a Deep-Learning-Based Earthquake Catalog in Central Myanmar

Shun Yang[1,2,3,4], Zhuowei Xiao[2,3], Shengji Wei[4,5], Yumei He[2], Chit Thet Mon[2,6], Guangbing Hou[2], Myo Thant[7,8], Kyaing Sein[6], and Mingming Jiang[2,3]

[1]Marine Science and Technology College, Zhejiang Ocean University, Zhoushan, China, [2]Key Laboratory of Earth and Planetary Physics, Institute of Geology and Geophysics, Chinese Academy of Sciences (CAS), Beijing, China, [3]University of Chinese Academy of Sciences, Beijing, China, [4]Asian School of the Environment, Nanyang Technological University, Singapore, Singapore, [5]Earth Observatory of Singapore, Nanyang Technological University, Singapore, Singapore, [6]Myanmar Geosciences Society, Yangon, Myanmar, [7]Department of Geology, Yangon University, Yangon, Myanmar, [8]Myanmar Earthquake Committee, Yangon, Myanmar

Key Points:

- We detect 1891 shallow earthquakes in Myanmar with a deep-learning-empowered pipeline, a 2-fold increase against the routine procedure
- N-S seismicity discrepancy is observed near the Kabaw Fault and may imply different responses to E-W shortening by the Indian subduction
- Low *b*-value derived from the new catalog on the middle Sagaing Fault indicates a high risk of destructive earthquakes

Supporting Information:

Supporting Information may be found in the online version of this article.

Correspondence to:

M. Jiang,
jiangmm@mail.iggcas.ac.cn

Citation:

Yang, S., Xiao, Z., Wei, S., He, Y., Mon, C. T., Hou, G., et al. (2024). New insights into active faults revealed by a deep-learning-based earthquake catalog in central Myanmar. *Geophysical Research Letters*, *51*, e2023GL105159. https://doi.org/10.1029/2023GL105159

Received 26 JUL 2023
Accepted 15 DEC 2023

Abstract Myanmar bears a high risk of destructive earthquakes, yet detailed seismicity catalogs are rare. We designed a deep-learning-based data processing pipeline and applied it to the data recorded by a large-aperture (~400 km) seismic array in central Myanmar to produce a high-resolution earthquake catalog. We precisely located 1891 earthquakes at shallow (<50 km) depth, a 2-fold increase compared to the traditional procedures. The new catalog reveals the Kabaw Fault seismicity disappears south of ~22.8°N, where the deeper (20–40 km) seismicity appears west of the southern Kabaw Fault. Such seismicity contrast along the strike of the Kabaw Fault possibly implies an along-strike change of deformation responses to the shortening process by the India plate oblique subduction. The middle segment of the Sagaing Fault is likely locked and prone to hosting large earthquakes according to the derived low *b*-value.

Plain Language Summary Myanmar is a highly seismically active region, yet fault geometry and activities remain poorly understood because of limited modern seismological investigations. Here, we designed a set of machine-learning algorithms to detect small earthquakes and determine their locations precisely. The seismic data are recorded by a temporary seismic network deployed in central Myanmar. We obtained twice as many earthquakes as the previous research used the regular procedure. Our improved earthquake data set unveils seismic activity changes along the Kabaw Fault through the changes in earthquake locations, depths, and magnitude-frequency relations. Kabaw Fault is an import boundary fault in the subduction system of the Indo-Burma Range. This subtle change was not previously observed but means a significant alternation in deformation style along the subduction strike. Moreover, our improved data set indicates that the Sagaing Fault, the most active fault in Myanmar, is prone to generating large earthquakes in the future. This implication warns the nearby populated cities, like Mandalay, of a significant megaquake threat.

1. Introduction

Myanmar, situated at the southeastern end of the Alpine-Himalayan earthquake belt, is highly susceptible to seismic hazards (Aung, 2015; Hurukawa & Maung, 2011; Sloan et al., 2017; Somsa-Ard & Pailoplee, 2013; Thant et al., 2012; Thein et al., 2009). The present-day tectonic activities in Myanmar are dominated by the northeastward oblique subduction of the Indian plate to its west, which results in a series of north-south trending active faults, especially the Sagaing Fault and the Kabaw Fault (Figure 1) (Sloan et al., 2017). The Kabaw Fault serves as the tectonic border between the Central Myanmar Lowland (CML) and the Indo-Burman Range (IBR) (Figure 1). Previous geodetic measurements suggested that the Kabaw Fault absorbs both thrust and strike-slip offsets caused by oblique subduction, and the associated seismic hazard could be underestimated (Oryan et al., 2023). However, the seismicity variation along the strike of the Kabaw Fault that accommodates tectonic deformation in the crust is poorly understood (Mallick et al., 2019; Maurin & Rangin, 2009; Mon et al., 2020; Steckler et al., 2016). Establishing a high-resolution regional earthquake catalog is vital for analyzing fault geometry and activity, as well as seismic hazards.

Recently, there has been a significant bloom of modern seismological observations in Myanmar and its surrounding regions (Witze, 2019), including the China-Myanmar Geophysical Survey of the Myanmar Orogen (CMGSMO) seismic network (Mon et al., 2020; Yang et al., 2022), Earth Observatory of Singapore-Myanmar

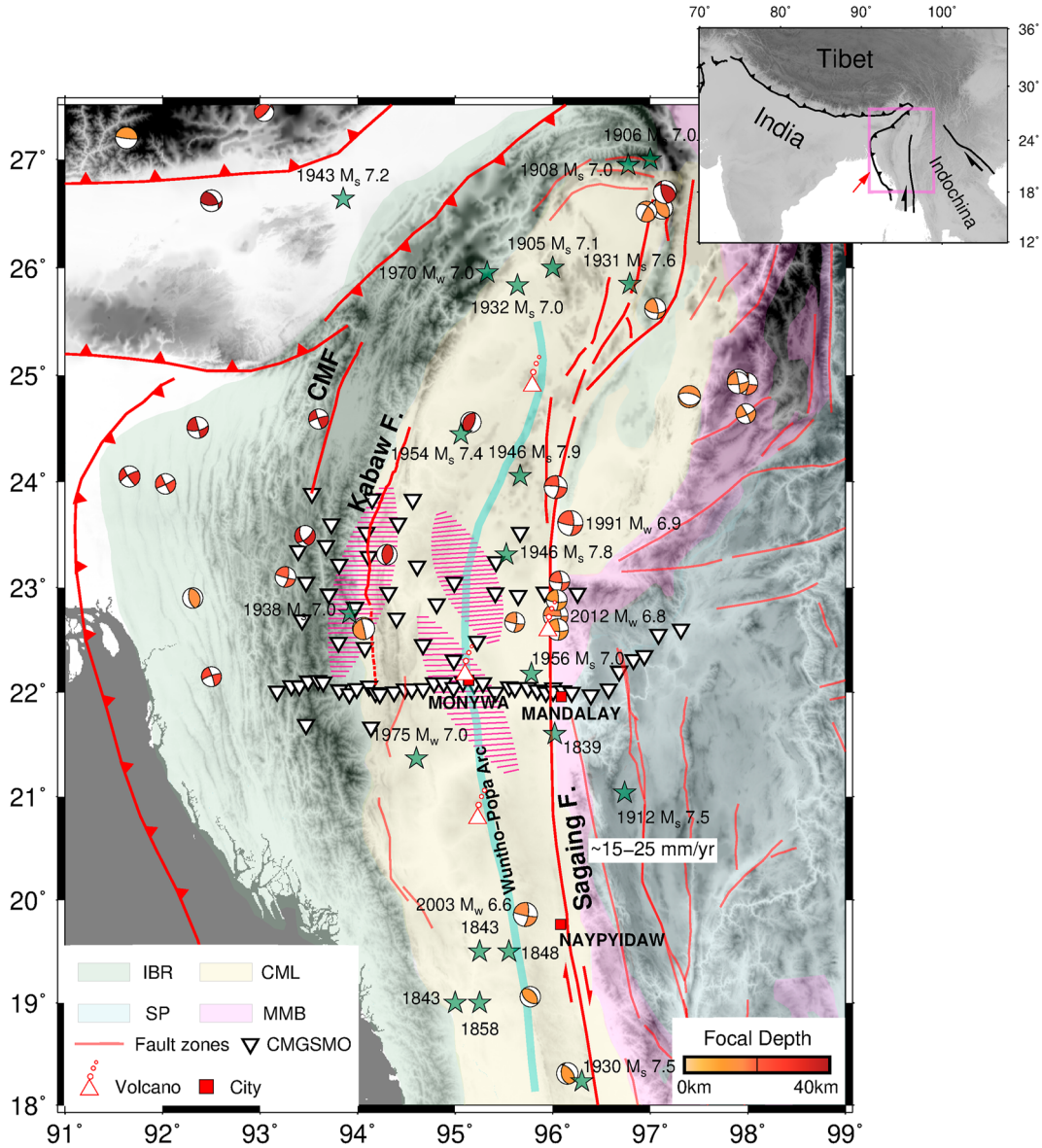

Figure 1. Overview of the Myanmar region, including the seismotectonic map of Myanmar and the distribution of the CMGSMO seismic array (white inverted triangles). The earthquakes with magnitudes larger than 7.0 are shown by green stars from Le Dain et al. (1984) and International Seismological Centre (ISC; Adams et al., 1982). Earthquake (Mw ≥ 5.5) focal mechanisms with depths shallower than 40 km are taken from the GCMT catalog (Ekström et al., 2005) for the period of 1976–2021. The magenta-shaded areas represent two NW-SE trending seismic zones in the CML and the Eastern Indo-Burma Ranges Seismic Zone in the IBR, discovered by Mon et al. (2020). The upper-right inset shows the location of our study area (purple rectangle). Abbreviations: SP, Shan Plateau; MMB, Mogok Metamorphic belt; CMF, Churachandpur-Mao Fault.

(EOS-Myanmar) seismic network (Fadil et al., 2021, 2023; X. Wang et al., 2019), TREMBLE seismic network (X. Wang et al., 2019), and the Myanmar National seismic network (MM; Thiam et al., 2017). This boost in seismic stations has highly enhanced the detection capacity of regional seismic networks, providing an excellent opportunity to better resolve and locate the seismicity. Mon et al. (2020) used the new seismic data recorded by the dense array of the CMGSMO to establish the first high-resolution catalog of local earthquakes in central Myanmar. Based on the earthquake distribution and focal mechanisms in the catalog, they identified a crustal seismic zone close to the Kabaw Fault and two seismic clusters beneath the sedimentary cover of the CML, and suggested the thrusting faults near the Kabaw Fault and the dextral strike-slip blind faults in the CML accommodate the deficiency of the oblique deformation (Mon et al., 2020). However, the relatively sparse distribution of earthquakes

around the Kabaw Fault zone hinders the precise determination of the fault geometry and activity. Moreover, the elongation of two seismic clusters stretching in the NW-SE direction does not match the near N-S striking tectonic units and major active faults. Therefore, further investigation is needed to acquire the elaborate variations of seismicity along the fault system relating to the subtle variations of fault geometry and stress status, which will help deepen our understanding of activity variations of the fault system and the changes in local tectonic deformation patterns.

Also note that, in Mon et al. (2020), the earthquakes were detected using the traditional STA/LTA method (Allen, 1978; Freiberger, 1963), and arrival times of regional earthquakes were manually picked. The STA/LTA method relies on hyperparameters and might neglect low signal-to-noise ratio (SNR) data, which could result in undetected of small-magnitude earthquakes. In contrast, the recent development of deep-learning-based earthquake detection and arrival time picking algorithms exhibited greater power to automatically and rapidly derive higher resolution and completeness earthquake catalogs that reveal new seismicity and fault features (e.g., Liu et al., 2020; Mousavi et al., 2020; Xiao et al., 2021). However, most of these neural network models were trained with seismic data sets acquired at local distances (e.g., <200 km in Chai et al. (2020), Liu et al. (2020), Mousavi et al. (2020), Zhu and Beroza (2019)). Therefore, they may not perform well when directly applied to the data recorded at greater distances (e.g., in our case, in central Myanmar, ∼400 km).

In this study, to maximize earthquake detection for the central Myanmar region to gain new insights into fault activity, we proposed a deep-learning-empowered, fully automatic data processing pipeline, named DEPALORE. We applied it to the 18-month seismic raw data used in Mon et al. (2020). The name DEPALORE (Figure S1 in Supporting Information S1) stands for five fundamental blocks in this pipeline: earthquake DEtection (EqT), Picking refinement (PickNet-TL), Association (REAL), LOcation (NonLinloc) and RElocation (HypoDD). The results show that the DEPALORE catalog contains much more well-resolved local events, which results in robust *b*-value estimations and reveals some new features for seismicity along the Kabaw Fault and within the CML compared to the manual catalog.

2. Tectonic Background

The Myanmar region consists of several north-south trending geological slivers, including the IBR and the CML attached to the Shan Platea, the margin of the Asian plate (Sloan et al., 2017). The IBR represents the accretionary prism of the subduction zone (Maurin & Rangin, 2009), separated from the CML by the Kabaw Fault. Geomorphology investigations revealed an east-dipping fault that traversed the eastern side of the Kabaw valley, which the Kabaw Fault was named after (Swe et al., 1972).

The CML comprises the fore-arc and back-arc basins separated by the Wuntho-Popa volcanic arc, which hosts several Quaternary volcanoes (e.g., Mt. Monywa and Mt. Popa; Than et al., 2017). The Monywa volcano has the most recent eruption records in the Holocene, which formed a series of maars (Belousov et al., 2018; Maury et al., 2004). Several large earthquakes struck the CML, suggesting the presence of active blind faults below it (Figure 1) (Fadil et al., 2021, 2023).

The Sagaing Fault, extending approximately 1,400 km, represents the tectonic boundary between the CML and the Shan Plateau. It serves as the primary fault zone that accommodates the majority of the strike-slip portion of the oblique convergence, with a slip rate of ∼15–25 mm/yr and accumulated slippage of 100–700 km (Curray, 2005; Swe, 1970; Tin et al., 2022; Tun & Watkinson, 2017).

3. Data and Methodology

To prepare the data for machine-learning-based earthquake detection, we utilized the same CMGSMO (Figure 1) raw data as in Mon et al. (2020). We built training, validation, and test data sets with the manual arrival picks reported in Mon (2021) and the associated seismograms. The training data set consists of ∼39,000 P and ∼28,500, and the validation data set consists of ∼2,000 P and ∼1,500 S. The test data set includes ∼5,000 P and ∼3,500 S.

The deep-learning-empowered fully automatic DEPALORE pipeline (see Text S2 in Supporting Information S1 for details) consists of five sequential steps (Figure S1 in Supporting Information S1): (a) initial automatic P and S wave arrival time detection using the original pre-trained EqT model (Mousavi et al., 2020); (b) arrival time picking refinement using the transfer learned PickNet model (J. Wang et al., 2019); (c) phase association and

initial event location determination using the Rapid Earthquake Association and Location method (REAL; Zhang et al., 2019); (d) precise earthquake absolute location inversion using NonLinLoc method (Lomax et al., 2009) and (e) high-resolution relative hypocenter relocation using the double-difference method (HypoDD; Waldhauser & Ellsworth, 2000).

The EqT model is an optimal solution for earthquake detection trained by data acquired at local distances, mostly less than 110 km. When applying EqT (see Table S1 in Supporting Information S1 for parameter setup) to a data set that covers the regional distance (e.g., ∼400 km in our case), we found that the EqT model remains powerful in detecting earthquakes, but with insufficient precision on phase picking due to the lack of regional phase patterns in the training data set (Figures S2 and S3 in Supporting Information S1). The phase patterns could change dramatically as the epicenter distance changes from ∼110 to ∼400 km. Arrival time picking refinement is thus necessary.

We applied the PickNet model (J. Wang et al., 2019), which has high phase picking accuracy at epicentral distances up to ∼1,000 km, to refine arrival time picks. The phase-picking results obtained from the EqT model were exploited to generate input time windows for the PickNet model. We further boost the performance of PickNet by transfer learning (TL) based on the manual data set, designated as PickNet-TL. To ensure the generalization of PickNet-TL and avoid overfitting, we applied data augmentation schemes to the training data set (Zhu et al., 2020). As a result, PickNet and PickNet-TL models significantly improve the accuracy of phase picking, in particular, the PickNet-TL model can achieve similar accuracy as human experts (Text S1, Figures S2 and S3 in Supporting Information S1).

With the refined arrival time picks from PickNet-TL, we employed a sequential earthquake association (REAL) and location methods (NonLinLoc and HypoDD) (see Text S2 in Supporting Information S1 for details) to establish a higher resolution and completeness DEPALORE catalog in contrast with that in Mon et al. (2020).

4. Results

4.1. Distribution of Earthquake

We applied the DEPALORE pipeline to the 18-month seismic raw data recorded by the CMGSMO array. The EqT model yielded ∼161,100 P and ∼161,400 S picks, which were then refined by the PickNet-TL model with outputs of ∼132,000 P and ∼134,900 S picks. The refined arrival times were injected into REAL and were associated with 2573 regional earthquakes with focal depths shallower than 50 km. These events' locations were further updated by NonLinLoc, resulting in 1891 events with magnitudes ranging from 0.1 to 5.8. The number of events in the NonLinLoc catalog is twice that of the manual catalog (849 events) (Figure S4 in Supporting Information S1; Mon et al., 2020). After the HypoDD relocation, the catalog retained 1508 earthquakes with magnitudes ranging from 0.5 to 5.3. We conducted the Jackknife uncertainty analysis for earthquake location. The result indicates that the absolute location uncertainties are 3.9, 3.6, and 5.3 km for longitude, latitude, and depth, respectively (Text S3, Figure S5 in Supporting Information S1).

Compared with the global catalog in Myanmar, both the DEPALORE and manual catalogs (Mon et al., 2020) demonstrate more compact earthquake clusters with roughly north-south elongated distributions in the IBR, as well as along the Kabaw and Sagaing Faults (Figure 2, Figures S6 and S7 in Supporting Information S1). The DEPALORE catalog contains 1292 more earthquakes and thus shows clearer cluster shapes than the manual catalog (Mon et al., 2020). Beneath the IBR, we observed an east-dipping seismic belt at a depth greater than ∼20 km. This seismic belt is located within the subducting Indian plate that was imaged as a high-velocity zone in the tomographic model (Figure 2; Zhang et al., 2021). Besides intra-slab seismicity, another nearly N-S trending earthquake cluster is observed in the overriding plate near the Kabaw Fault. This seismicity cluster corresponds to the previously identified Eastern Indo-Burma Ranges Seismic Zone (EIBRSZ) by Mon et al. (2020). Based on the clustering of hypocenter distribution in our catalog, we further divided the seismicity near the Kabaw Fault into two sections bounded by the latitude of ∼22.8°N (Figure 3). In the northern section, earthquakes roughly distribute along the Kabaw Fault and primarily concentrate around a depth of 20 km. The southern section exhibits ∼30 km westward offset from the surface trail of the Kabaw Fault at greater depths of 20–40 km.

Beneath the CML, the incremental earthquakes in the new catalog fill the previous seismic gap between the Ye-U Fault zone and the Kani Fault zone as defined by Mon et al. (2020), and we recognized clearer N-S trending of two seismic clusters within the domains of fore- and back-arc basins, respectively (Figure 2 and Figure S6 in

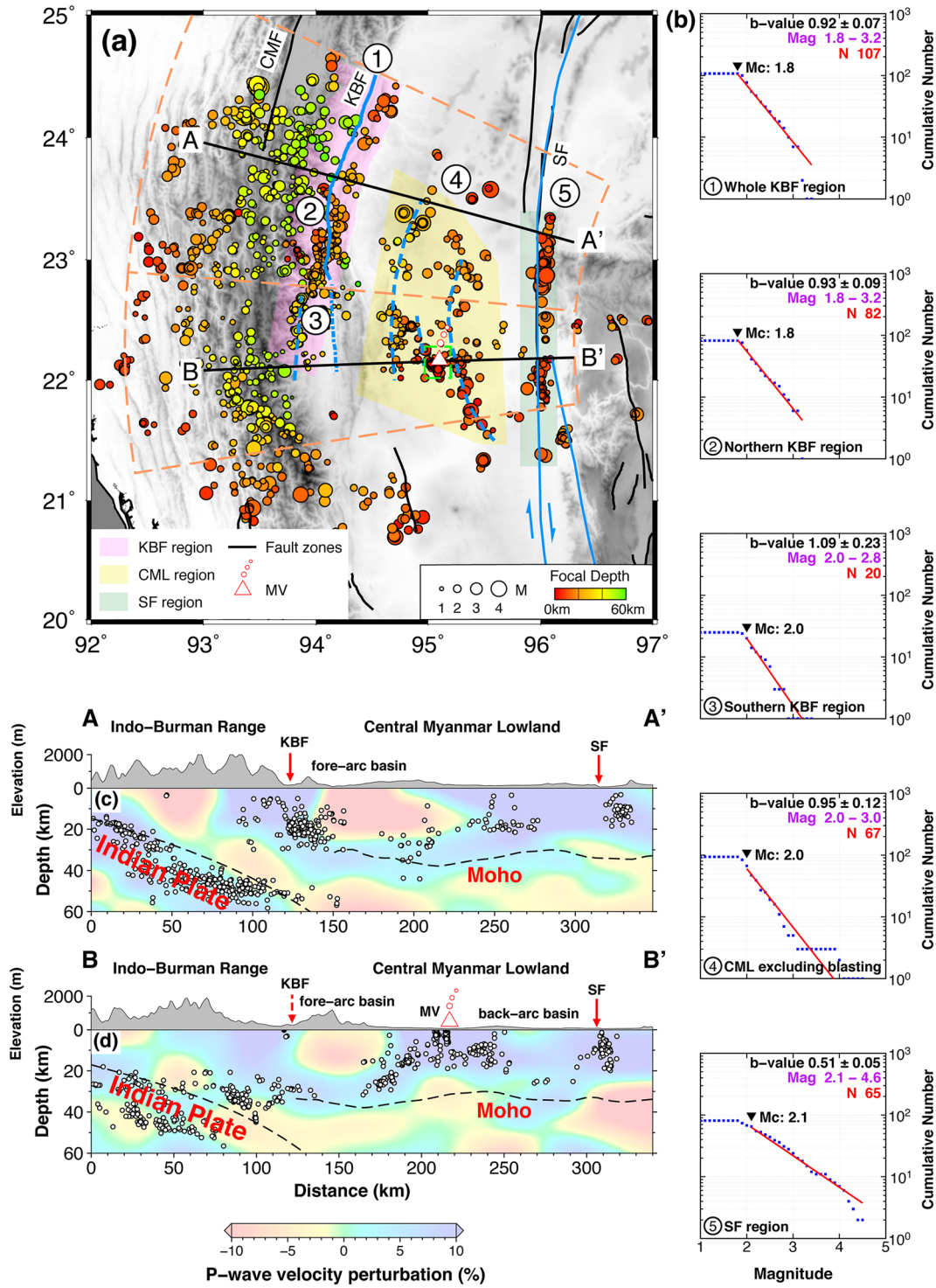

Figure 2. (a) The distribution of relocated shallow earthquakes in central Myanmar from the DEPALORE catalog. The relocated earthquakes are colored by depth and sized by magnitude. The tectonic sketch of central Myanmar is plotted as background. (b) The cumulative frequency-magnitude distribution (FMD) for different sub-regions. The sub-regions are indicated by circled numbers and shaded areas with different colors in subplot (a). The blasting-related seismicity is distributed at the region contoured by the green dashed line in subplot (a). The numbers in purple and red represent the magnitude range and the number of earthquakes used for *b*-value calculation. (c, d) Transect views of the earthquake distributions. The colored background is P-wave velocity perturbations from Zhang et al. (2021). The positions of profiles A-A′ and B-B′ are shown in subplot (a) with black lines. The earthquakes within the orange dashed box are projected to the profiles. Abbreviations: MV, Monywa Volcano; KBF, Kabaw Fault; SF, Sagaing Fault.

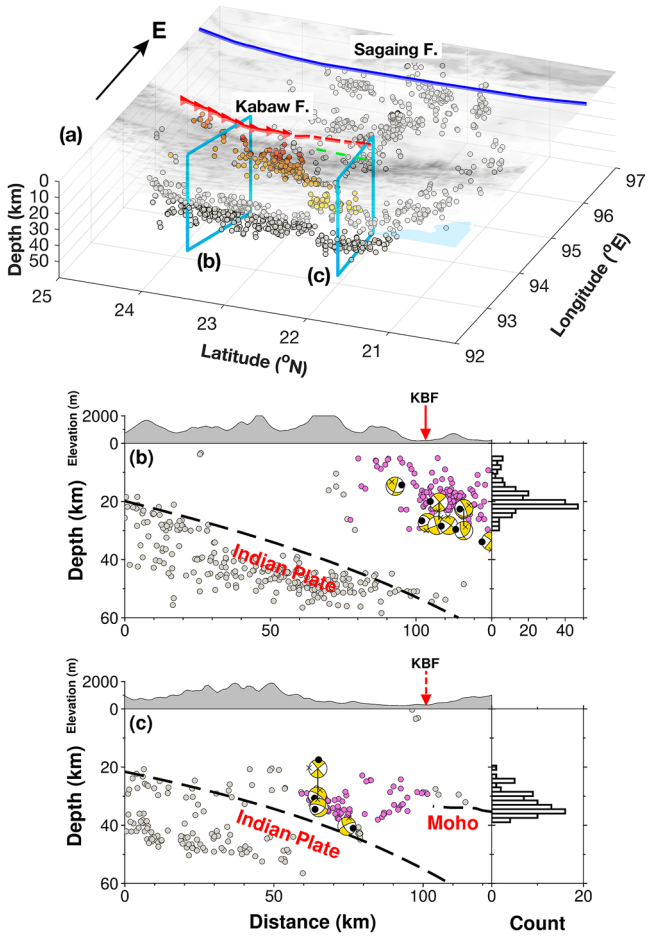

Figure 3. (a) 3-D perspective and (b, c) Transect views for the distribution of relocated shallow earthquakes in the vicinity of the Kabaw Fault. The earthquakes near the Kabaw Fault shown in Figure 2a are highlighted as purple circles, and the rest are set as gray. The cyan boxes in subplot (a) denote the vertical sections in the transect views (b, c). In subplot (b, c), the focal mechanisms are obtained from Mon et al. (2020) and GCMT (1976–2021). The histograms indicate the depth distribution of the earthquakes related to the northern and southern sections of the Kabaw Fault region.

Supporting Information S1). The strikes of these blind active faults coincide with the N-S trending tectonic characteristics of the Myanmar region (Licht et al., 2019). By comparing the seismicity with the high-resolution tomography model in the CML (Zhang et al., 2021), we noticed that nearly all earthquakes are located beneath the thick sedimentary layers in the bedrock (Figures 2c and 2d). Notably, our new catalog reveals the presence of two seismicity swarms occurring at an extremely shallow depth range of 0–5 km near the Monywa volcano (Figure 2). These swarm events have nearly identical origin time of 8:00 a.m. (Figure S8 in Supporting Information S1) and are distributed to two mining sites (Figure S9 in Supporting Information S1), which suggests that these events were more likely produced by artificial blasting for mining work rather than natural earthquakes. High agreement between swarm events and mining sites also indicates a high-resolution horizontal location of the DEPALORE catalog (with an uncertainty of ∼2 km). At the eastern boundary of the CML, earthquakes are concentrated along the Sagaing Fault at a depth range of 0–25 km (Figure 2).

4.2. Spatial Variation of *b*-Value

Enough of earthquakes in our new catalog allows for the derivation of *b*-values for different fault systems and the comparison of their fault activities. Here, we divided the studied area into three sub-regions and calculated the background *b*-values for the whole study region and each sub-region (Text S4 in Supporting Information S1). We used the maximum-likelihood method to estimate *b*-values (Aki, 1965). During this process, dependent earthquakes such as foreshocks and aftershocks were removed (Uhrhammer, 1986). The *b*-values after declustering for different sub-regions are nearly consistent with those before declustering (Figure 2 and Figure S10 in Supporting Information S1).

The DEPALORE catalog has a completeness magnitude (M_c) of 1.8 (M_L), which is a considerable improvement compared to the manual catalog with M_c of 2.1 (M_L) (Mon et al., 2020; Figure S4b in Supporting Information S1). The *b*-value for the entire catalog is estimated as 0.76, nearly equal to that derived from the manual catalog (Mon et al., 2020), which verifies the robustness and stability of *b*-value estimation even with the inclusion of smaller earthquakes in the DEPALORE catalog. The northern and southern sections of the seismic zone near the Kabaw Fault have *b*-values of 0.93 and 1.09, respectively (Figure 2). After removing the blasting-related seismicity, the *b*-value of the remaining seismicity beneath CML is estimated to be 0.95 (Figure 2), which is slightly larger than that near the Kabaw Fault. High seismic signal attenuation due to the thick sediments beneath CML (Zhang et al., 2021) may cause the *b*-value underestimation because small events are more likely to be undetected. The seismicity along the Sagaing Fault shows an even lower *b*-value of 0.51. The standard deviations of the *b*-value for most sub-regions are within 0.12, except for the southern section of the Kabaw Fault due to the lack of earthquakes (Figure 2).

Notably, our *b*-values are estimated from earthquakes within a limited magnitude range over a relatively short observation period (Figure 2). Magnitude spans of less than three units may lead to an overestimation of the *b*-value (Marzocchi et al., 2020). However, we find that the *b*-value of the short-term DEPALORE catalog closely aligns with those of global long-term catalogs for central Myanmar (Figure S11 in Supporting Information S1). For the seismicity of sub-regions, the *b*-values of these long-term catalogs are hardly calculated due to the high uncertainty in the location of earthquakes and the limited number of earthquakes. We thus suppose that the *b*-values of our new catalog might provide insight into the long-term seismicity in central Myanmar.

5. Discussion

Based on our results of earthquake relocation, the Sagaing Fault exhibits a slightly eastward dipping at a depth range of 0–25 km (Figures 2c and 2d). The maximum focal depth is much deeper than the estimated locking depth

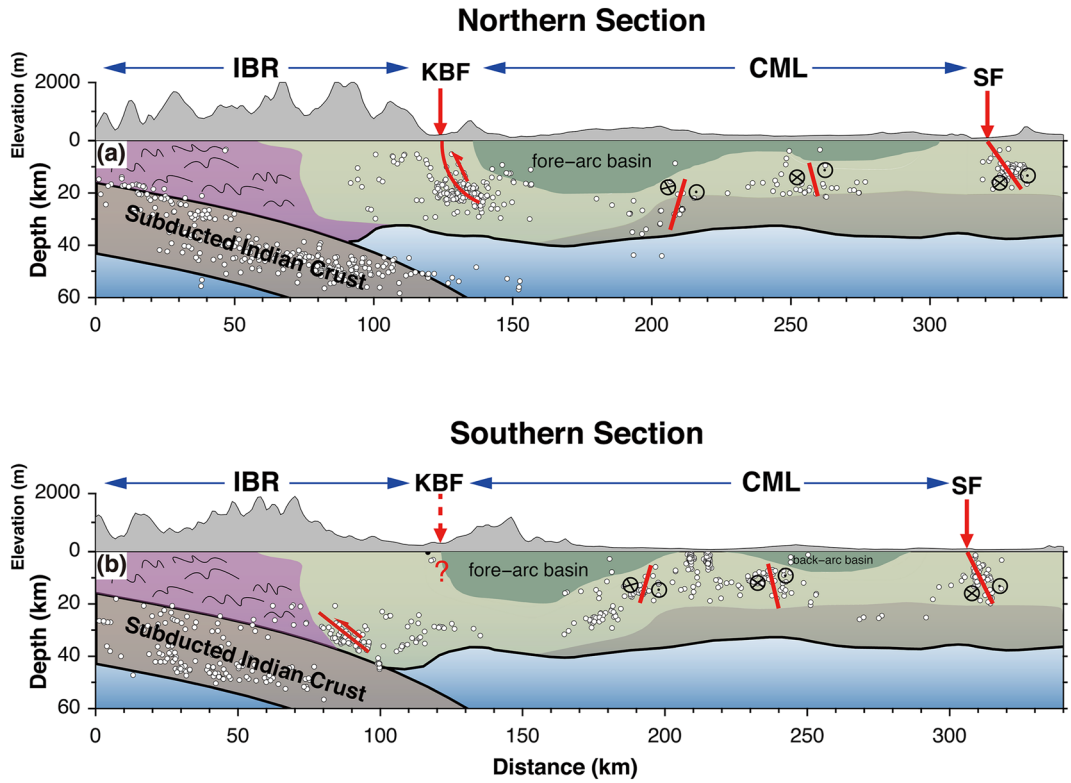

Figure 4. Schematic diagrams of the active fault systems in the hanging wall of the Indo-Burman subduction. Architecture variations along tectonic strike are illustrated by the contrastive northern (a) and southern (b) sections.

of 10 km by campaign GNSS observations (Tin et al., 2022), suggesting a possible deeper seismogenic zone. The Sagaing Fault seismicity yields a low *b*-value of 0.51 ± 0.05, which is consistent with the fact that most destructive earthquakes occurred on the Sagaing Fault (Figure 1; Y. Wang et al., 2014). Considering the influence of the narrow magnitude range (Marzocchi et al., 2020), the *b*-value of the Sagaing Fault seismicity may be lower. The lower *b*-value on the Sagaing Fault indicates a high level of stress status (Scholz, 2015), which coincides with the GNSS observations that the Sagaing Fault accommodates a majority of the strike-slip partition of the highly oblique convergence between the Indian plate and Sunda plate (Mallick et al., 2019; Steckler et al., 2016). Analogous to the *b*-value analysis on the San Andreas Fault (Wyss et al., 2004), low *b*-value suggests this segment of the Sagaing Fault is highly locked at present, as also shown in the GNSS observations (Tin et al., 2022). Thus, a large earthquake tends to occur in this segment of the Sagaing Fault in the future.

The most distinct feature revealed by our catalog is that the earthquake cluster within the Kabaw Fault region exhibits remarkably different features between the northern and southern sections, which are bounded at the latitude of ~22.8°N (Figure 3). The earthquakes in the northern section are mainly distributed in the upper to middle crust roughly along the outcrops of the Kabaw Fault, featuring a *b*-value of 0.93 (Figure 2). We attributed this seismicity to the activity of the Kabaw Fault according to the spatial coherence between the epicenter distribution and the fault outcrops. By contrast, the earthquakes in the southern section concentrate in the lower crust, featuring a relatively high *b*-value of 1.09 (Figure 2). Their surface project notably deviates from the outcrops of the proposed southward extension of the Kabaw Fault (Figure 3; Y. Wang et al., 2014). The *b*-value mapping based on long-term catalogs hinted at the *b*-value variations along the strike of the Kabaw Fault (Bora et al., 2018). Likewise, the longstanding geomorphic features are obviously different between the regions adjacent to the northern and southern Kabaw Fault (Figure 4). The earthquakes in both sections exhibit consistent thrust focal mechanisms with E-W oriented *P* axes (Figure 3). We, therefore, prefer that the sudden seismicity change at the latitude of ~22.8°N near the Kabaw Fault might imply an along-strike variation of deformation accommodation to the E-W shortening (Figure 4). Indeed, we can hardly rule out the possibility that this seismicity change is a short-term phenomenon due to the relatively short observation period. The Kabaw Fault segment south of ~22.8°N might be locked in the upper/middle crust and is being loaded by lower crustal aseismic deformation

accompanied by microseismicity. Recent GNSS modeling results suggest that the northern Kabaw Fault is locked and active and argue that it is capable of hosting large earthquakes (Oryan et al., 2023). However, the slip rate and locking status of the southern Kabaw Fault remain unclear. Long-term regional seismic observation and more GNSS observations are needed to better understand the seismicity of the Kabaw Fault region.

6. Conclusions

Compared to the earthquake catalog derived from manual arrival time picks, we built a catalog with better resolution and completeness for central Myanmar by applying a deep-learning-empowered fully automatic pipeline. This pipeline is efficiently constructs earthquake catalogs in large-scale (∼400 km) regions. The newly obtained DEPALORE catalog contains 2-fold more earthquakes and is of a lower completeness magnitude than the previous manual one. Based on the novel catalog, we find new insights into the seismicity and active faults in central Myanmar as follows:

1. A roughly N-S trending earthquake cluster was traced near the Kabaw Fault. Northern and southern sections of this cluster are distinct in proximity to the Kabaw Fault, focal depths, and *b*-values. The different seismicity between the northern and southern sections likely suggests the different deformation accommodation to the E-W shortening process by the India plate oblique subduction.
2. Beneath the CML, we re-depicted two approximately north-south oriented seismic clusters, corresponding to blind fault systems. Their strikes coincide with the stretching direction of the tectonic slivers in Myanmar.
3. The middle segment of the Sagaing Fault exhibits a low *b*-value of 0.51 ± 0.05, suggesting high effective stress and present locked status. Therefore, this fault segment is capable of hosting large earthquakes that pose a severe threat to adjacent population centers.

Data Availability Statement

The seismograms used in this study are available at the WDC for Geophysics, Beijing (Yang et al., 2023).

Acknowledgments
We gratefully acknowledge the researchers and colleagues at the Seismic Array Laboratory, Institute of Geology and Geophysics, CAS, for their efforts to install and maintain the CMGSMO seismic network. We thank Yukuan Chen for sharing the simplified module to run NonLinLoc. We thank Chenyu Li and Wardah Fadil for valuable discussions. Plots were generated using Generic Mapping Tools (GMT) (Wessel & Smith, 1998) and Matplotlib (Hunter, 2007). This work was supported by the National Natural Science Foundation of China (Grants 42130308, 42030309, 91755214).

References

Adams, R. D., Hughes, A. A., & McGregor, D. M. (1982). Analysis procedures at the International Seismological Centre. *Physics of the Earth and Planetary Interiors*, *30*(2–3), 85–93. https://doi.org/10.1016/0031-9201(82)90093-0

Aki, K. (1965). *Maximum likelihood estimate of b in the formula logN= a-bM and its confidence limits* (Vol. 43, pp. 237–239). Bulletin of Earthquake Research Institute of the University of Tokyo, Tokyo University.

Allen, R. V. (1978). Automatic earthquake recognition and timing from single traces. *Bulletin of the Seismological Society of America*, *68*(5), 1521–1532. https://doi.org/10.1785/bssa0680051521

Aung, H. H. (2015). *Myanmar earthquake history*. Myanmar Engineering Society.

Belousov, A., Belousova, M., Zaw, K., Streck, M. J., Bindeman, I., Meffre, S., & Vasconcelos, P. (2018). Holocene eruptions of Mt. Popa, Myanmar: Volcanological evidence of the ongoing subduction of Indian Plate along Arakan Trench. *Journal of Volcanology and Geothermal Research*, *360*(2), 126–138. https://doi.org/10.1016/j.jvolgeores.2018.06.010

Bora, D. K., Borah, K., Mahanta, R., & Borgohain, J. M. (2018). Seismic b-values and its correlation with seismic moment and Bouguer gravity anomaly over Indo-Burma ranges of northeast India: Tectonic implications. *Tectonophysics*, *728–729*, 130–141. https://doi.org/10.1016/j.tecto.2018.01.001

Chai, C., Maceira, M., Santos-Villalobos, H. J., Venkatakrishnan, S. V., Schoenball, M., Zhu, W., et al. (2020). Using a deep neural network and transfer learning to bridge scales for seismic phase picking. *Geophysical Research Letters*, *47*(16), e2020GL088651. https://doi.org/10.1029/2020GL088651

Curray, J. R. (2005). Tectonics and history of the Andaman Sea region. *Journal of Asian Earth Sciences*, *25*(1), 187–232. https://doi.org/10.1016/j.jseaes.2004.09.001

Ekström, G., Dziewoński, A. M., Maternovskaya, N. N., & Nettles, M. (2005). Global seismicity of 2003: Centroid-moment-tensor solutions for 1087 earthquakes. *Physics of the Earth and Planetary Interiors*, *148*(2–4), 327–351. https://doi.org/10.1016/j.pepi.2004.09.006

Fadil, W., Lindsey, E. O., Wang, Y., Maung, P. M., Luo, H., Swe, T. L., et al. (2021). The January 11, 2018, M_w 6.0 Bago-Yoma, Myanmar Earthquake: A shallow thrust event within the deforming Bago-Yoma range. *Journal of Geophysical Research: Solid Earth*, *126*(7), e2020JB021313. https://doi.org/10.1029/2020JB021313

Fadil, W., Wei, S., Bradley, K., Wang, Y., He, Y., Sandvol, E., et al. (2023). Active faults revealed and new constraints on their seismogenic depth from a high-resolution regional focal mechanism catalog in Myanmar (2016–2021). *Bulletin of the Seismological Society of America*, *113*(2), 613–635. https://doi.org/10.1785/0120220195

Freiberger, W. F. (1963). An approximate method in signal detection. *Quarterly of Applied Mathematics*, *20*(4), 373–378. https://doi.org/10.1090/qam/139498

Hunter, J. D. (2007). Matplotlib: A 2D graphics environment. *Computing in Science & Engineering*, *9*(3), 90–95. https://doi.org/10.1109/MCSE.2007.55

Hurukawa, N., & Maung, P. M. (2011). Two seismic gaps on the Sagaing Fault, Myanmar, derived from relocation of historical earthquakes since 1918. *Geophysical Research Letters*, *38*(1), L01310. https://doi.org/10.1029/2010GL046099

Le Dain, A. Y., Tapponnier, P., & Molnar, P. (1984). Active faulting and tectonics of Burma and surrounding regions. *Journal of Geophysical Research*, *89*(B1), 453–472. https://doi.org/10.1029/JB089iB01p00453

Licht, A., Dupont-Nivet, G., Win, Z., Swe, H. H., Kaythi, M., Roperch, P., et al. (2019). Paleogene evolution of the Burmese forearc basin and implications for the history of India-Asia convergence. *Bulletin of the Geological Society of America*, *131*(5–6), 730–748. https://doi.org/10.1130/B35002.1

Liu, M., Zhang, M., Zhu, W., Ellsworth, W. L., & Li, H. (2020). Rapid characterization of the July 2019 Ridgecrest, California, earthquake sequence from raw seismic data using machine-learning phase picker. *Geophysical Research Letters*, *47*(4), e2019GL086189. https://doi.org/10.1029/2019GL086189

Lomax, A., Michelini, A., & Curtis, A. (2009). Earthquake location, direct, global-search methods. In R. A. Meyers (Ed.), *Encyclopedia of complexity and systems science* (pp. 2449–2473). Springer New York. https://doi.org/10.1007/978-0-387-30440-3

Mallick, R., Lindsey, E. O., Feng, L., Hubbard, J., Banerjee, P., & Hill, E. M. (2019). Active convergence of the India-Burma-Sunda plates revealed by a new continuous GPS network. *Journal of Geophysical Research: Solid Earth*, *124*(3), 3155–3171. https://doi.org/10.1029/2018JB016480

Marzocchi, W., Spassiani, I., Stallone, A., & Taroni, M. (2020). How to be fooled searching for significant variations of the b-value. *Geophysical Journal International*, *220*(3), 1845–1856. https://doi.org/10.1093/gji/ggz541

Maurin, T., & Rangin, C. (2009). Structure and kinematics of the Indo-Burmese Wedge: Recent and fast growth of the outer wedge. *Tectonics*, *28*(2), TC2010. https://doi.org/10.1029/2008TC002276

Maury, R. C., Pubellier, M., Rangin, C., Wulput, L., Cotten, J., Socquet, A., et al. (2004). Quaternary calc-alkaline and alkaline volcanism in an hyper- oblique convergence setting, central Myanmar and western Yunnan. *Bulletin de la Societe Geologique de France*, *175*(5), 461–472. https://doi.org/10.2113/175.5.461

Mon, C. T. (2021). *New insight into active faults and subducted Indian plate beneath central Myanmar, based on seismic activity and focal mechanisms analysis*. University of Chinese Academy of Sciences. Wanfang Data.

Mon, C. T., Gong, X., Wen, Y., Jiang, M., Chen, Q. F., Zhang, M., et al. (2020). Insight into major active faults in central Myanmar and the related geodynamic sources. *Geophysical Research Letters*, *47*(8), e2019GL086236. https://doi.org/10.1029/2019GL086236

Mousavi, S. M., Ellsworth, W. L., Zhu, W., Chuang, L. Y., & Beroza, G. C. (2020). Earthquake transformer—An attentive deep-learning model for simultaneous earthquake detection and phase picking. *Nature Communications*, *11*(1), 3952. https://doi.org/10.1038/s41467-020-17591-w

Oryan, B., Betka, P. M., Steckler, M. S., Nooner, S. L., Lindsey, E. O., Mondal, D., et al. (2023). New GNSS and geological data from the Indo-Burman subduction zone indicate active convergence on both a locked megathrust and the Kabaw Fault. *Journal of Geophysical Research: Solid Earth*, *128*(4), e2022JB025550. https://doi.org/10.1029/2022JB025550

Scholz, C. H. (2015). On the stress dependence of the earthquake b value. *Geophysical Research Letters*, *42*(5), 1399–1402. https://doi.org/10.1002/2014GL062863

Sloan, R. A., Elliott, J. R., Searle, M. P., & Morley, C. K. (2017). Active tectonics of Myanmar and the Andaman Sea. *Geological Society Memoir*, *48*(1), 19–52. https://doi.org/10.1144/M48.2

Somsa-Ard, N., & Pailoplee, S. (2013). Seismic hazard analysis for Myanmar. *Journal of Earthquake and Tsunami*, *7*(4), 1350029. https://doi.org/10.1142/S1793431113500292

Steckler, M. S., Mondal, D. R., Akhter, S. H., Seeber, L., Feng, L., Gale, J., et al. (2016). Locked and loading megathrust linked to active subduction beneath the Indo-Burman ranges. *Nature Geoscience*, *9*(8), 615–618. https://doi.org/10.1038/ngeo2760

Swe, W. (1970). Rift-features at the Sagaing–Tagaung ridge. In *Proceedings of the 5th Burma research congress*.

Swe, W., Thacpaw, C., Thaung, N. T., & Nyunt, K. (1972). Geology of the Chindwin basin of the central belt of Burma. In *7th Burma research congress*.

Than, N. M., Khin, K., & Thein, M. (2017). Cretaceous geology of Myanmar and Cenozoic geology in the Central Myanmar Basin. *Geological Society Memoir*, *48*(1), 143–167. https://doi.org/10.1144/M48.7

Thant, M., Ngal, N. L., Tun, S. T., Thein, M., Swe, W., & Myint, T. (2012). *Seismic hazard assessment for Myanmar*. Myanmar Earthquake Committee and Myanmar Geoscience Society.

Thein, M., Myint, T., Tun, S. T., & Swe, T. L. (2009). Earthquake and Tsunami hazard in Myanmar. *Journal of Earthquake and Tsunami*, *3*(2), 43–57. https://doi.org/10.1142/S1793431109000482

Thiam, H. N., Htwe, Y. M. M., Kyaw, T. L., Tun, P. P., Min, Z., Htwe, S. H., et al. (2017). A report on upgraded seismic monitoring stations in Myanmar: Station performance and site response. *Seismological Research Letters*, *88*(3), 926–934. https://doi.org/10.1785/0220160168

Tin, T. Z. H., Nishimura, T., Hashimoto, M., Lindsey, E. O., Aung, L. T., Min, S. M., & Thant, M. (2022). Present-day crustal deformation and slip rate along the southern Sagaing fault in Myanmar by GNSS observation. *Journal of Asian Earth Sciences*, *228*, 105125. https://doi.org/10.1016/j.jseaes.2022.105125

Tun, S. T., & Watkinson, I. M. (2017). The Sagaing Fault, Myanmar. *Geological Society Memoir*, *48*(1), 413–441. https://doi.org/10.1144/M48.19

Uhrhammer, R. A. (1986). Characteristics of northern and central California seismicity. *Earthquake Notes*, *57*(1), 21.

Waldhauser, F., & Ellsworth, W. L. (2000). A double-difference earthquake location algorithm: Method and application to the northern Hayward fault, California. *Bulletin of the Seismological Society of America*, *90*(6), 1353–1368. https://doi.org/10.1785/0120000006

Wang, J., Xiao, Z., Liu, C., Zhao, D., & Yao, Z. (2019). Deep learning for picking seismic arrival times. *Journal of Geophysical Research: Solid Earth*, *124*(7), 6612–6624. https://doi.org/10.1029/2019JB017536

Wang, X., Wei, S., Wang, Y., Maung Maung, P., Hubbard, J., Banerjee, P., et al. (2019). A 3-D shear wave velocity model for Myanmar region. *Journal of Geophysical Research: Solid Earth*, *124*(1), 504–526. https://doi.org/10.1029/2018JB016622

Wang, Y., Sieh, K., Tun, S. T., Lai, K. Y., & Myint, T. (2014). Active tectonics and earthquake potential of the Myanmar region. *Journal of Geophysical Research: Solid Earth*, *119*(4), 3767–3822. https://doi.org/10.1002/2013JB010762

Wessel, P., & Smith, W. H. F. (1998). New, improved version of generic mapping tools released. *Eos, Transactions American Geophysical Union*, *79*(47), 579. https://doi.org/10.1029/98eo00426

Witze, A. (2019). Quake-prone Myanmar primed for seismic scrutiny. *Nature*, *566*(7743), 166–167. https://doi.org/10.1038/d41586-019-00501-6

Wyss, M., Sammis, C. G., Nadeau, R. M., & Wiemer, S. (2004). Fractal dimension and b-value on creeping and locked patches of the San Andreas Fault near Parkfield, California. *Bulletin of the Seismological Society of America*, *94*(2), 410–421. https://doi.org/10.1785/0120030054

Xiao, Z., Wang, J., Liu, C., Li, J., Zhao, L., & Yao, Z. (2021). Siamese earthquake transformer: A pair-input deep-learning model for earthquake detection and phase picking on a seismic array. *Journal of Geophysical Research: Solid Earth*, *126*(5), e2020JB021444. https://doi.org/10.1029/2020jb021444

Yang, S., Liang, X., Jiang, M., Chen, L., He, Y., Mon, C. T., et al. (2022). Slab remnants beneath the Myanmar terrane evidencing double subduction of the Neo-Tethyan Ocean. *Science Advances*, *8*(34). https://doi.org/10.1126/sciadv.abo1027

Yang, S., Xiao, Z., Wei, S., He, Y., Mon, C. T., Hou, G., et al. (2023). Detailed earthquake catalog in central Myanmar and seismic waveform data from China-Myanmar Geophysical Survey in the Myanmar Orogen (CMGSMO) project [Dataset]. WDC for Geophysics. https://doi.org/10.12197/2023GA010

Zhang, G., He, Y., Ai, Y., Jiang, M., Mon, C. T., Hou, G., et al. (2021). Indian continental lithosphere and related volcanism beneath Myanmar: Constraints from local earthquake tomography. *Earth and Planetary Science Letters*, *567*, 116987. https://doi.org/10.1016/j.epsl.2021.116987

Zhang, M., Ellsworth, W. L., & Beroza, G. C. (2019). Rapid earthquake association and location. *Seismological Research Letters*, *90*(6), 2276–2284. https://doi.org/10.1785/0220190052

Zhu, W., & Beroza, G. C. (2019). PhaseNet: A deep-neural-network-based seismic arrival-time picking method. *Geophysical Journal International*, *216*(1), 261–273. https://doi.org/10.1093/gji/ggy423

Zhu, W., Mousavi, S. M., & Beroza, G. C. (2020). Seismic signal augmentation to improve generalization of deep neural networks. *Advances in Geophysics*, *61*, 151–177. https://doi.org/10.1016/bs.agph.2020.07.003

References From the Supporting Information

Efron, B. (1980). *The jackknife, the bootstrap, and other resampling plans*. (Technical Report No. 63). Stanford University.

Hutton, L. K., & Boore, D. M. (1987). The ML scale in Southern California. *Bulletin of the Seismological Society of America*, *77*(6), 2074–2094. https://doi.org/10.1785/BSSA0770062074

Shi, Y., & Bolt, B. A. (1982). The standard error of the magnitude-frequency b value. *Bulletin of the Seismological Society of America*, *72*(5), 1677–1687. https://doi.org/10.1785/bssa0720051677

Wiemer, S., & Wyss, M. (2000). Minimum magnitude of completeness in earthquake catalogs: Examples from Alaska, the western United States, and Japan. *Bulletin of the Seismological Society of America*, *90*(4), 859–869. https://doi.org/10.1785/0119990114

Wyss, M., Schorlemmer, D., & Wiemer, S. (2000). Mapping asperities by minima of local recurrence time: San Jacinto-Elsinore fault zones. *Journal of Geophysical Research*, *105*(B4), 7829–7844. https://doi.org/10.1029/1999jb900347

Zheng, T., He, Y., Ding, L., Jiang, M., Ai, Y., Mon, C. T., et al. (2020). Direct structural evidence of Indian continental subduction beneath Myanmar. *Nature Communications*, *11*(1), 1944. https://doi.org/10.1038/s41467-020-15746-3